Phytochemistry Letters 40 (2020) 26–36

Contents lists available at ScienceDirect

Phytochemistry Letters

journal homepage: www.elsevier.com/locate/phytol

Comparative analyses of metabolic fingerprint integrated with cytotoxic activity and in silico approaches of the leaves extract of *Spondias mombin* L. and *Spondias tuberosa* Arr. Cam. from Northeast, Brazil

Jhonyson Arruda Carvalho Guedes [a,b], Yuri Gomes Santiago [b], Licia dos Reis Luz [a,b], Maria Francilene Souza Silva [c], Christiane Mendes Cassimiro Ramires [d], Maria Auxiliadora Coelho de Lima [e], Viseldo Ribeiro de Oliveira [e], Cláudia do Ó Pessoa [c], Kirley Marques Canuto [b], Edy Sousa de Brito [b], Marcelo F. Lima [f], Ricardo Elesbão Alves [h], Davila Zampieri [g], Ronaldo Ferreira do Nascimento [a], Guilherme Julião Zocolo [b,*]

[a] *Departamento de Química Analítica e Físico-Química, Universidade Federal do Ceará, Av. Humberto Monte, s/n - Pici, Fortaleza, CE, CEP 60455-760, Brazil*
[b] *Embrapa Tropical Agroindustry. Rua Dra. Sara Mesquita, 2270 - Pici, Fortaleza, CE, CEP 60020-181, Brazil*
[c] *Núcleo de Pesquisa e Desenvolvimento de Medicamentos - NPDM, Universidade Federal do Ceará, Rua Coronel Nunes de Mello 1000, CEP 60420-275 Fortaleza, CE, Brazil*
[d] *Empresa Paraibana de Pesquisa, Extensão Rural e Regularização Fundiária - EMPAER - PB, Brazil*
[e] *Embrapa Semiárido, Rodovia BR-428, Km 152, Zona Rural, CEP 56302-970, Petrolina, PE, Brazil*
[f] *Universidade Estadual Paulista (Unesp), Instituto de Biociências, Letras e Ciências Exatas (IBILCE), Câmpus São José do Rio Preto, Brazil*
[g] *Departamento de Química Orgânica e Inorgânica, Universidade Federal do Ceará, Av. Humberto Monte, s/n - Pici, CEP 60455-760, Fortaleza, CE, Brazil*
[h] *Embrapa Alimentos e Territórios - Maceió, AL, Brazil*

ARTICLE INFO

Keywords:
Metabolomics
Yellow mombin
Umbu
Chemometrics
High-resolution mass spectrometry
Liquid chromatography

ABSTRACT

Spondias species are a relevant source of natural-bioactive compounds in Brazilian folk medicine, and its biological potential has not been explored. Thus, this study aimed to determine the metabolomic fingerprint of *Spondias mombin* and *Spondias tuberosa* leaves based on the use of reversed-phase liquid chromatography coupled to a high-resolution mass spectrometer (UPLC-HRMS). The analysis by UPLC-HRMS allowed the annotation of 31 metabolites. The multivariate analysis allowed us to identify the biomarkers responsible for the distinction between species. Also, we correlate the biomarkers of *S. mombin* and *S. tuberosa* as supposed responsible for the difference in the degree of cytotoxicity between them. The *in silico* evaluation was performed to give more consistency to the correlation between biomarkers and cytotoxicity, which were compared to commercial drugs. Therefore, this study showed that *S. mombin* has the potential to become an input for the pharmaceutical industry as a source of raw material that can positively impact the sectors of agricultural production.

1. Introduction

Among the species of the genus *Spondias*, we can highlight the commercial importance of *Spondias mombin* L. (Anacardiaceae family) and *Spondias tuberosa* Arr. Cam. (Anacardiaceae family). Its fruits are marketed *in natura* or processed in the form of pulps, juices and other food products. In addition to commercial use, there is also considerable literature on use of species of this genus as medicinal plants, being used for the treatment of infectious disorders and also as abortive (Agra et al., 2007; Hajdu and Hohmann, 2012; Pereira et al., 2015).

In traditional medicine, in several regions of the world, leaves, barks, and stems of *Spondias mombin* (popularly known as yellow mombin) are used for the treatment of infectious disorders, mainly diarrhea, and dysentery. In the *in vitro* studies, the aqueous and ethanolic extracts of *S. mombin* leaves inhibited bacterial growth, is this the first report of the validation of the popular use of this species as an antibacterial agent (Ajao et al., 1985). Since then, several properties have been attributed to extracts from *S. mombin*.

Studies reveal that the hydroalcoholic extract of *S. mombin* inhibits the replication of Herpes simplex and coxsakie B viruses, responsible for

* Corresponding author.
E-mail address: guilherme.zocolo@embrapa.br (G.J. Zocolo).

https://doi.org/10.1016/j.phytol.2020.09.003
Received 12 May 2020; Received in revised form 5 August 2020; Accepted 1 September 2020
Available online 23 September 2020

painful mouth ulcers. The active compounds against these viruses were identified as geraniin, galoylgeraniine, and two esters of caffeine (Corthout et al., 1991). Besides, recent studies reported in the literature have indicated that the hydroethanolic extract from *S. mombin* exhibits antioxidant and anti-inflammatory activities, in addition, these extracts have anxiolytic and antidepressant actions (Cabral et al., 2016; Gomes et al., 2020; Sampaio et al., 2018).

Spondias tuberosa (popularly known as umbu), the ethnopharmacological study identified its uses for the treatment of some pathologies, among them diabetes, inflammations, uterine cramps, and stomach pains (Neto et al., 2010). The fruits of the *S. tuberosa* present pronounced antioxidant activity and free radical sequestration, which can be attributed to the presence of phenolic compounds and vitamin C, also, there are reports of the presence of flavonoids, anthocyanins, and carotenoids. Other compounds well known for their therapeutic properties have also been detected *S. tuberosa*, such as gallic acid, chlorogenic acid, protocatechuic acid, *p*-coumaric acid, vanillyl acid, and ferulic acid (Dias et al., 2019; Gomes et al., 2013; Zeraik et al., 2016). In the literature, there are also reports that the hexane extract from *S. tuberosa* showed a potent cytotoxic activity, showing inhibition of cell growth (Guedes et al., 2020).

Scientific studies have supported most of the medicinal uses that people in various parts of the world make of plants of the genus *Spondias*. Besides, pharmacological properties not reported by the population were also observed in experimental models. The leaves extract from *S. tuberosa* and *S. mombin* showed antiviral activity against the dengue virus type 2. This fact was associated with the presence of ellagic acid, flavonoids, quercetin, and rutin in the extracts (Silva et al., 2011).

Many of the pharmacological properties of the genus *Spondias* are attributed to the phenolic compounds (tannins and flavonoids), mostly present in leaves. However, other secondary metabolites may also contribute to these activities, since vitamin C, saponins, alkaloids, terpenes, and carotenoids have been identified in these species (Bataglion et al., 2015; Pereira et al., 2015; Zeraik et al., 2016). The evidence of these compounds associated with the popular knowledge of anti-inflammatory and healing effects of this species becomes promising for investigation and discovery of new drugs.

Also, because many activities have been studied and proven, and research has shown low toxicity in experimental models *in vivo* (Tomás-Barberán and Clifford, 2000), it is justified the continuity of other research on species of this genus. Besides, the literature lacks further information on the chemical profile of these species, associated with cytotoxicity activity of the pulp, leaves, and bark of the species. Thus, the metabolomic approach combined with ultra-performance liquid chromatography-quadrupole time-of-flight mass spectrometry (UPLC-QTOF-MS^E) is a powerful tool for analyzing the profile of metabolites present in *S. mombin* (yellow mombin) and *S. tuberosa* leaves (umbu) (González-Riano et al., 2020; Liu et al., 2019; Pezzatti et al., 2020).

In this sense, the present work proposes to perform the metabolomic study of *S. mombin* and *S. tuberosa* leaves, using reversed-phase liquid chromatography coupled to a high-resolution mass spectrometer (UPLC-HRMS), together with chemometric analyzes and *in vitro* cytotoxic assays different cancer cell lines. Also, comparisons, using molecular orbitals calculations, from the major components of *S. mombin* and commercially available drugs, active against leukemia and other cancer cell lines, have detailed out the chemical similarities between those compounds. In this way, it will be possible to trace the metabolic fingerprint of the *S. mombin* and *S. tuberosa* leaves, as well as to correlate them with the cytotoxic activity.

2. Materials and methods

2.1. Samples, reagents and chemicals

Samples of *S. mombin* and *S. tuberosa* leaves were collected at the Germoplasm Active Bank of Empresa Paraibana de Pesquisa, Extensão Rural e Regularização Fundiária - EMPAER, in the city of João Pessoa, in the state of Paraíba, Brazil, and at the Umbuzeiro Germplasm Bank - UGB, Caatinga Experimental Field, at Embrapa Semiárido, in Petrolina, PE, Brazil, respectively.

Sample collection was carried out so that the respective species (*S. mombim* and *S. tuberosa*) were studied in sample pool systems, this study a mixture of leaves from twenty accessions collected by species was performed ($N = 20$).

The samples were subjected to the liquid nitrogen quenching process, later they were submitted dried in a circulating air oven for three days at 40 °C. Subsequently, the dry plant material was ground and packed in transparent plastic bags, properly identified and protected from moisture and light.

After drying the plant material (*S. mombin* and *S. tuberosa*) the twenty accessions collected to each specie were mixed and homogenized, forming a pool of samples, this final mixture was subdivided into five sub-samples that were analyzed separately to test the reproducibility and repeatability parameters of the analytical method. This large pool of individuals was determined so that there was a comprehensive profile of metabolites representative of the genetic variability present in the active germplasm bank.

Water was purified using a Milli-Q Integral Water Purification System (Millipore, Bedford, MA, USA). Ethanol (96%) and hexane (95%) are purchased from Tedia (Rio de Janeiro, RJ, Brazil), and the acetonitrile (LC-MS grade) was supplied by Tedia (Fairfield, Ohio, EUA). Formic acid (purity ~ 98%), Dimethyl sulfoxide (DMSO) and 3-(4,5-dimethyl-2-thiazol)-2,5-diphenyl-2H-tetrazolium bromide (MTT) were purchased from Sigma-Aldrich (Life Science).

The tumor cells used, PC3 (prostate), HL60 (leukemia), SNB-19 (astrocytoma), MCF-7 (breast), B16F10 (melanoma) and L929 (non-tumor) were donated by the National Cancer Institute, NCI-USA, cultured in RPMI 1640 medium, supplemented with 10% fetal bovine serum and 1% antibiotics, kept in an oven at 37 °C and atmosphere containing 5% CO_2.

2.2. Extraction methodology for UPLC analysis

The extracts were obtained by liquid-liquid partition using ultrasound. Initially, a 50 mg amount of the dried plant leaf samples was weighed into a test tube. Subsequently, 4 mL of 95% hexane was added and the mixture was vortexed for 1 min. The extraction of the non-polar compounds was performed in an ultrasonic bath for 20 min with fixed power of 135 W. Then, 4 mL of hydroethanolic solution (7:3) was added. The mixture was vortexed for 1 min and sonicated for 20 min. Thereafter, the test tubes were centrifuged to decant the undissolved plant material at 3000 rpm for 10 min. At the end of the procedure, a 1 mL aliquot of the lower polar phase (hydroethanolic) was removed, and this aliquot was filtered on a 0.22 μm PTFE filter. The filtered aliquot was collected in vials and sent for analysis in UPLC-QTOF-MS^E (Chagas--Paula et al., 2015; Guedes et al., 2020, 2018; Nehme et al., 2008). The extraction procedure was done in quintuplet for the two species and the extraction blank in triplicate, $N = 13$ extractions.

2.3. Extraction methodology for the analysis of cytotoxicity activity

Extraction for biological analysis occurred similarly to the procedure for UPLC-QTOF-MS^E analysis, as described in section 2.2. However, at the end of the procedure, instead of withdrawing a 1 mL aliquot of the hydroethanolic phase, 3 mL was withdrawn, to obtain a sufficient mass of at least 10 mg for cytotoxic testing. The extracts were dried in a rotary evaporator and lyophilized.

2.3.1. Methodology for evaluation of cytotoxic potential in vitro

For the analyzes of the cytotoxic potential, all the extracts were evaluated *in vitro* using the MTT assay against cancer cell lines: PC3

(prostate), HL60 (leukemia), SNB-19 (astrocytoma), MCF-7 (breast) and B16F10 (melanoma). The selectivity of the compounds toward a normal proliferating cell line was investigated using the cell line L929 (non-tumor) after 72 h of drug exposure. All cancer cell lines were maintained in RPMI 1640 medium. The L929 cell was cultivated under standard conditions in DMEM with Earle's salts. All culture media were supplemented with 10% fetal bovine serum, 2 mmol L^{-1} glutamine, 100 IU mL^{-1} penicillin, 100 mg mL^{-1} streptomycin at 37 °C with 5% CO_2. In cytotoxicity experiments, cells were plated in 96-well plates (0.1×10^6 cells/well for PC3, SNB-19, B16F10, MCF-7 and L929 cells, HL60 cells 0.3×10^6 cells/well). All tested compounds were dissolved with DMSO. The final concentration of DMSO in the culture medium was kept constant (0.1%, v/v).

The cell viability was determined through the reduction of the yellow dye MTT to a blue formazan product, as described by Mosmann (1983). At the end of the incubation time (72 h), the plates were centrifuged and the medium was replaced with fresh medium (200 mL) containing 0.5 mg mL^{-1} MTT. Three hours later, the MTT formazan product was dissolved in DMSO (150 μL) and the absorbance was measured using a multiplate reader (DTX 880 Multimode Detector, Beckman Coulter, Inc. Fullerton, California, EUA). The extract effect was quantified as the percentage of the control absorbance of the reduced dye at 595 nm. The results were analyzed according to the mean ± standard deviation of the mean of the percentage of growth inhibition (GI, %) of the cell. Each sample was tested in triplicate in two independent experiments. Values were computed using GraphPad Prism® 5.0 program.

2.4. Metabolomics analysis - Reversed-phase UPLC-QTOF-MS^E conditions

The analyzes were performed in an Acquity UPLC (Waters, Milford, MA, USA) chromatographic system, coupled to a quadrupole/time of flight (QTOF, Waters, Milford, MA, USA). Chromatographic runs were performed on a Waters Acquity UPLC BEH (150 mm x 2.1 mm, 1.7 μm), fixed temperature 40 °C. The binary gradient elution system consisted of 0.1% formic acid in water (A) and 0.1% formic acid in acetonitrile (B). The UPLC elution conditions were optimized as follows: linear gradient from 2 to 95% B (0-15 min), 100% B (15-17 min), 2% B (17.01), 2% (17.02-19.01 min), a flow of 0.4 mL min^{-1}, and a sample injection volume of 3 μL.

The chemical profile of samples was performed by coupling the Waters ACQUITY UPLC system to the QTOF mass spectrometer (Waters, Milford, MA, USA) with the electrospray ionization interface in negative ionization mode (ESI-). The ESI- mode was acquired in the range of 110-1180 Da in MS and in the range of 50-1180 Da in MS^2, fixed source temperature at 120 °C, desolvation temperature 350 °C, desolvation gas flow of 500 L h^{-1}, extraction cone of 0.5 V, the capillary voltage of 2.6 kV. Leucine enkephalin was used as a lock mass. The spectrometer operated with MS^E centroid programming using a tension ramp from 20 to 40 V. The instrument was controlled by Masslynx 4.1 software (Waters Corporation).

2.5. Metabolite annotation

The data generated by the UPLC-QTOF-MS^E analyzes were processed using MassLynx software version 4.1. The comparison of all the peaks in the mass chromatogram was made based on a tolerance of ±0.05 min for the retention time and ±0.05 Da for the exact mass. All possible molecular formulas were deduced (elements C, H, O, and tolerance of 10 ppm) using the *Elemental Composition* tool from MassLynx.

It is important to note that the metabolic fingerprint of the species was established through the MS^E spectra, by the dereplication of the 31 compounds that were annotated according to data from the literature based on chemotaxonomy.

2.6. Data processing and statistical analysis

To discriminate the chemical profiles obtained through the UPLC-QTOF-MS^E of the different species, all data were processed by the MarkerLynx statistical software. Subsequently, the multivariate analysis was performed, where the PCA (principal components analysis) and the OPLS-DA (orthogonal partial least squares discriminant analysis) were performed. The multivariate analysis was performed under the following conditions: retention time 0.80 to 17.00 min, a mass range of 110 to 1180 Da, tolerance of masses 0.05 Da, and elimination of noise at the level of 5.

For the analysis of the data, a list of peak intensities detected using the retention time pair (t_R) and mass data (m/z) was used as the identifier of each peak. An arbitrary identification was assigned to each of these t_R-m/z pairs based on their elution order. The ion intensities for each detected peak were normalized against the sum of the peak intensities within that sample using MarkerLynx. The compounds were considered the same when they matched their t_R and m/z values (Sousa et al., 2017).

The data set was mean-centered, and the Pareto scale method was used to generate the PCA. The data composing the peak number (t_R-m/z pair), sample name, and ion intensity were analyzed by principal component analysis (PCA) and orthogonal partial least squares discriminant analysis (OPLS-DA) using the MarkerLynx software. The mean-centered calculates the average spectrum of the data set and subtracts the average of each spectrum, aiming to focus the floating part of the data instead of the original value. The Pareto scale measures each variable by the square root of its standard deviation, amplifying the contribution of metabolites of lower concentration (Ni et al., 2008; van den Berg et al., 2006).

2.7. Theoretical calculations

The structures chlorogenic acid, geraniin, myricetin-3-*O*-rhamnoside, and the commercial substances used for comparison purposes paclitaxel and doxorubicin were downloaded from PubChem (Kim et al., 2016) database with the respectively PubChem CID: 1794427, 3001497, 56843093, 36314 and 31703. The structures were optimized from molecular mechanics UFF (Rappe et al., 1992) force field to ab initio DFT/ωB97X-D/6-311++G(d,p) including dispersion corrections (Chai and Head-Gordon, 2008). All ab initio calculation was performed in a solution using C-PCM (Barone and Cossi, 1998; Cossi et al., 1996; Tomasi et al., 2005) implicit model for each interaction. Optimizations were followed by harmonic frequency calculations to obtain vibrational, rotational, and translational contributions to the free energy. For optimized structures, single-point energy calculations were performed using DFT/ωB97X-D/6-311++G(d,p) basis set also in solution via C-PCM to evaluate the charge of the system using the geodesic (Spackman) (Spackman, 1996) approach. All ab initio calculations were performed using GAMESS version 1 May 2013 (R1) program system (Schmidt et al., 1993). The visualization and analysis of the results were done using MacMolplt program (Bode and Gordon, 1998). All final optimized structures are present in the supplementary material.

3. Results and discussion

3.1. Analysis of the metabolic fingerprint of *S. mombin* and *S. tuberosa* leaves

The ultra-performance liquid chromatography coupled to the mass spectrometer with electrospray ionization source and quadrupole/time-of-flight analyzers (UPLC-QTOF-MS^E) was of great relevance for obtaining the chemical profiles of the hydroethanolic extracts from *S. mombin* and *S. tuberosa*. In view, the power to analyze small amounts of sample and at low levels of concentration, in rapid analyzes with obtaining high resolution spectra. Thus, the combination of UPLC with

mass spectrometry (UPLC-QTOF-MS^E), was an essential factor in the metabolite annotation.

The chemical profile of the *S. mombin* and *S. tuberosa* leaves was established by analyzing the negative mode (ESI-) chromatograms, as shown in Fig. 1, together with the chromatograms the mass spectra were analyzed. Besides, it is important to note that the metabolite annotation was based on studies that used samples of the same genus and species, genus, or family of the samples studied. To facilitate further manipulation of the data, the peaks displayed in the chromatograms were consecutively numbered according to the elution order (Table 1). In Table 1, it is possible to observe 43 compounds detected, with 31 metabolites annotated in the samples. Also associated with metabolites are their deprotonated ions [M-H]- and their ions fragments, as well as the error in parts per million (ppm) and its possible molecular formula. In the Supplementary Material it is possible to find a more detailed description of the metabolites annotation in the extracts from the leaves of *S. mombin* and *S. tuberosa*.

In general, the metabolic profiles of the *S. mombin* and *S. tuberosa* sample sets are quite similar, with metabolites of different chemical classes being noted, such as: phenolic acids, flavonoids, tannins, galotanins, elargitanines and some anacardic acids. However, it is also possible to observe some differences, in which they can be better evidenced and visualized with the multivariate analysis to be presented below.

3.2. Multivariate analysis

3.2.1. Principal Component Analysis (PCA)

The PCA was initially used to reduce the high-dimensional data set in a two-dimensional or three-dimensional score chart without losing important information. The scores and loadings graphs resulting from the PCA were used to investigate the relationship of the identified compounds with the analyzed samples, in order to verify possible groupings (Ni et al., 2008).

In the identification of compounds present in the leaves of *S. mombin* and *S. tuberosa*, it was possible to verify that the analyzed samples present differences regarding their metabolic composition. To support this observation, PCA was used. Thus, it was conceived by the pre-processed data, this technique allows the visualization of the data generated by the metabolic study of the *S. mombin* and *S. tuberosa* species, based on the similarities and differences inherent in the samples. Thus, those samples that have similar metabolic composition tend to cluster.

From the 3D PCA graph (Fig. 2) it is possible to verify that there is an indication of systematic trends among *S. mombin* and *S. tuberosa* species since it is possible to visualize the formation of two groups.

3.2.2. OPLS-DA and S-Plot analysis

The PCA made it possible to separate and distinguish the metabolomic fingerprint of the *S. mombin* and *S. tuberosa* species in two distinct groups. Thus, to determine the responsible variables, chemical markers, separation and consequent differentiation of groups of samples, the OPLS-DA associated with the S-Plot dispersion charts are used in the data set.

In this context, the OPLS-DA model was applied to the data from the UPLC-QTOF-MS^E to compare the groups of samples. The t_R-*m/z* values served as the basis for identifying or attempting to identify the potential biomarkers responsible for the classification and separation of the samples.

By analyzing the OPLS-DA score graph (Fig. 3 (a)) between the samples of the *S. mombin* and *S. tuberosa* leaves, it is possible to verify the clear separation of the two groups of samples. To evaluate the accuracy and reliability of the OPLS-DA model, two parameters were used: the variable R2Y, called explained variation and the variable Q2, called predicted variation. In summary, R2Y provides a measure of model fit for the original data, while Q2 provides an internal measure of

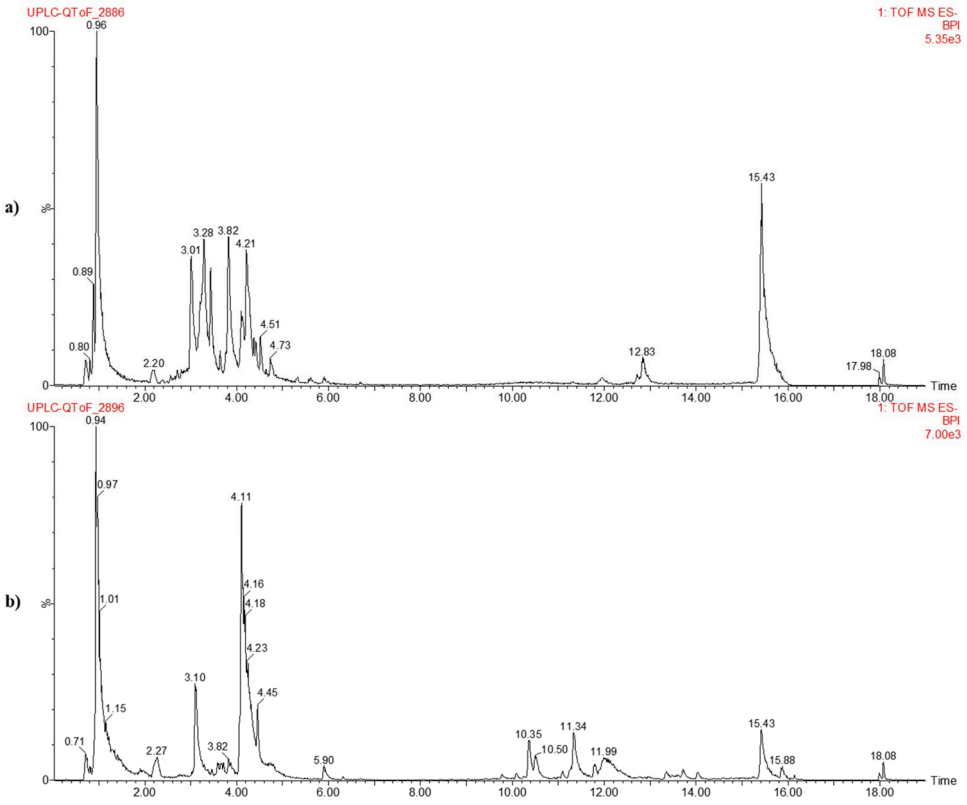

Fig. 1. Chromatogram obtained in the UPLC-QTOF-MS^E system in negative mode (ESI-) of the hydroethanolic extracts of the leaves from the: (a) *S. mombin* and (b) *S. tuberosa*.

Table 1
Metabolite annotation in samples of *Spondias mombin* (yellow mombin) and *Spondias tuberosa* (umbu).

Peak	t_R (min)	[M-H]- observed	[M-H]- calculated	Fragments of ions (MS/MS)	Molecular formula	Error (ppm)	Metabolite annotation	*S. mombin*	*S. tuberosa*	References
1	0.89	341.1084	341.1084	89.0253; 179.0508	$C_{12}H_{22}O_{11}$	0.0	sucrose	+	+	(Farag et al., 2014)
2	0.96	189.0026	189.0035	-	$C_6H_6O_7$	−4.8	not identified	+	+	-
3	2.20	315.0726	315.0716	108.0205; 109.0261; 153.0205	$C_{13}H_{16}O_9$	0.3	dihydroxybenzoic acid hexoside	+	+	(Engels et al., 2012)
4	2.98	353.0883	353.0873	191.0536; 179.0346; 127.0387; 93.0352; 85.0258	$C_{16}H_{18}O_9$	−2.0	chlorogenic acid (3-caffeoylquinic acid)	+		(Engels et al., 2012)
5	3.09	369.0406	369.0399	-	$C_{22}H_9O_6$	1.9	not identified		+	-
6	3.28	951.0728	951.0740	169.0121; 300.9928; 933.0704	$C_{41}H_{28}O_{27}$	−1.3	geraniin	+		(Kumar et al., 2015)
7	3.32	633.0721	633.0728	275.0136; 300.9921; 463.0549; 481.0700	$C_{27}H_{22}O_{18}$	−1.1	corilagin	+	+	(Kumar et al., 2015)
8	3.37	635.0850	635.0884	125.0153; 169.0037; 313.0535; 465.0733	$C_{27}H_{24}O_{18}$	−5.4	trigaloyl glucose		+	(Kumar et al., 2015)
9	3.43	1109.0990	1109.0979	-	$C_{22}H_{46}O_{50}$	1.0	not identified	+		-
10	3.47	387.1656	387.1655	207.0122	$C_{18}H_{28}O_9$	0.3	tuberonic acid hexoside		+	(Kumar et al., 2015)
11	3.54	457.0776	457.0771	169.0077; 305.0776	$C_{22}H_{18}O_{11}$	1.1	epigallocatechin-3-*O*-gallate		+	(Dou et al., 2007)
12	3.60	169.0136	169.0137	125.0209	$C_7H_6O_5$	−0.6	gallic acid	+		(Engels et al., 2012)
13	3.70	625.1405	625.1405	301.0172; 463.0570	$C_{27}H_{30}O_{17}$	0.0	quercetin-*O*-dihexoside	+	+	(Hanhineva et al., 2008)
14	3.81	383.0614	383.0614	-	$C_{16}H_{16}O_{11}$	0.0	not identified		+	-
15	3.85	953.0920	953.0896	935.0901; 633.0782; 463.0527	$C_{41}H_{30}O_{27}$	2.5	galloyl-bis-HHDP-glucose	+		(Silva et al., 2016)
16	3.99	787.0969	787.0994	169.0055; 465. 0557; 617.0544; 635.1483	$C_{34}H_{28}O_{22}$	−3.2	tetra-*O*-galloyl-glucoside	+	+	(Dorta et al., 2014)
17	4.02	609.1454	609.1456	151.0046; 179.9985; 257.0696; 271.0286; 300.0203; 301.0291	$C_{27}H_{30}O_{16}$	−0.2	quercetin rhamnosyl hexoside	+	+	(Engels et al., 2012)
18	4.12	609.1465	609.1456	151.0047; 271.0229; 300.0204; 301.0304; 343.0400	$C_{27}H_{30}O_{16}$	1.5	quercetin-3-*O*-rutinoside (rutin)		+	(Engels et al., 2012)
19	4.19	300.9972	300.9984	229.0009	$C_{14}H_6O_8$	−4.0	ellagic acid	+		(Cabral et al., 2016; Fracassetti et al., 2013)
20	4.25	463.0880	463.0877	150.9999; 179.0036; 271.0275	$C_{21}H_{20}O_{12}$	0.6	myricetin-3-*O*-rhamnoside	+	+	(Cunha et al., 2017)
21	4.28	463.0871	463.0877	272.0222; 301.0347	$C_{21}H_{20}O_{12}$	−1.3	quercetin-3-*O*-galactoside	+	+	(Erşan et al., 2016)
22	4.37	463.0891	463.0877	179.0049; 271.0242; 300.9987	$C_{21}H_{20}O_{12}$	3.0	quercetin-3-*O*-glucoside	+	+	(Erşan et al., 2016)
23	4.41	981.1262	981.1268	-	$C_{36}H_{38}O_{32}$	−0.6	not identified	+		-
24	4.45	609.1454	609.1456	193.0835; 271.0090; 300.0305	$C_{27}H_{30}O_{16}$	−0.3	rhamnetin hexosyl pentoside		+	(Engels et al., 2012)
25	4.50	593.1509	593.1506	255.0142; 284.0307; 285.0398	$C_{27}H_{30}O_{15}$	0.5	kaempferol deoxyhexosyl hexoside		+	(Engels et al., 2012)
26	4.52	433.0762	433.0771	255.0310; 271.0261; 300.0264; 301.0125	$C_{20}H_{18}O_{11}$	−2.1	quercetin-3-*O*-xyloside	+		(Schieber et al., 2003)
27	4.58	433.0756	433.0771	255.0297; 271.0261; 300.0275; 301.0098	$C_{20}H_{18}O_{11}$	−3.5	quercetin-3-*O*-arabinopyranoside	+		(Schieber et al., 2003)
28	4.66	433.0750	433.0771	255.0325; 271.0284; 300.0245; 300.9988	$C_{20}H_{18}O_{11}$	−4.8	quercetin-3-*O*-arabinofuranoside	+		(Schieber et al., 2003)
29	4.68	593.1512	593.1506	255.0273; 284.0290; 285.0376	$C_{27}H_{30}O_{15}$	1.0	kaempferol-3-*O*-rutinoside		+	(Engels et al., 2012)
30	4.72	615.0988	615.0986	169.0203; 287.0917; 469.8464	$C_{28}H_{24}O_{16}$	0.3	myricitrin-*O*-gallate		+	(Abu-reidah et al., 2015)
31	4.74	451.1032	451.1029	-	$C_{24}H_{20}O_9$	0.7	not identified	+		-
32	5.91	301.0350	301.0348	151.0022; 191.0171; 271.0193	$C_{15}H_9O_7$	0.7	quercetin	+	+	(Abu-reidah et al., 2015)
33	10.36	397.1324	397.1346	-	$C_{15}H_{25}O_{12}$	−5.5	not identified		+	-
34	10.49	675.3683	675.3686	-	$C_{44}H_{51}O_6$	−0.4	not identified		+	-
35	11.34	593.2791	593.2809	-	$C_{27}H_{45}O_{14}$	−3.0	not identified		+	-
36	11.79	653.3777	653.3783	-	$C_{49}H_{50}O$	−0.9	not identified		+	-
37	12.06	577.2653	577.2649	-	$C_{30}H_{41}O_{11}$	0.7	not identified		+	-
38	12.83	385.2385	385.2379	-	$C_{24}H_{34}O_4$	1.6	not identified	+		-
39	15.33	369.2430	369.2430	183.0168; 325.2550	$C_{24}H_{34}O_3$	0.0	(17:3)-anacardic acid	+	+	(Erşan et al., 2016)
40	15.43	371.2586	371.2586	107.0494; 119.0497; 327.2541	$C_{24}H_{36}O_3$	0.0	(17:2)-anacardic acid	+	+	(Erşan et al., 2016)
41	15.85	319.2274	319.2273	275.2350	$C_{20}H_{32}O_3$	0.3	(13:0)-anacardic acid		+	(Erşan et al., 2016)
42	15.95	345.2439	345.2430	301.2579	$C_{22}H_{34}O_3$	2.6	(15:1)-anacardic acid		+	(Erşan et al., 2016)
43	16.98	373.2776	373.2743	106.0412; 329.2853	$C_{24}H_{38}O_3$	8,8	(17:1)-anacardic acid		+	(Erşan et al., 2016)

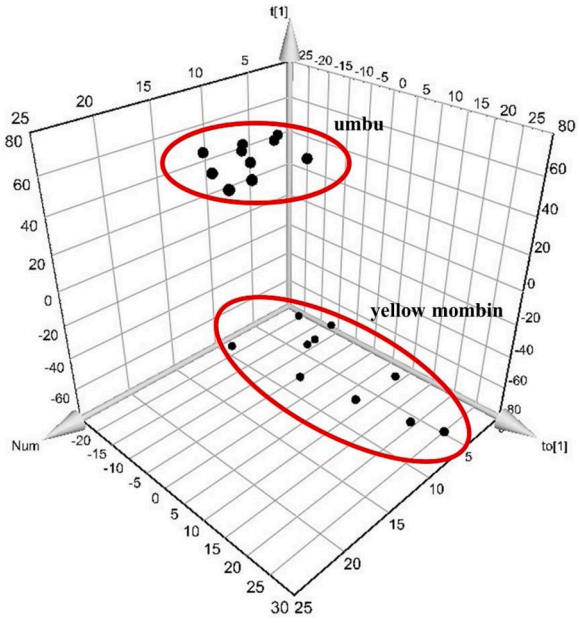

Fig. 2. Principal Component Analysis (PCA) in 3D of the hydroethanolic extracts of the leaves from the *S. mombin* and *S. tuberosa*, analyzed by UPLC-QTOF-MS^E.

consistency between the original and predictive data of the cross-validation. Models with parameters R2Y and Q2 close to 1 are considered excellent, although values above 0.5 are accepted when the components of the samples present high complexity (Wold et al., 2001).

Thus, the OPLS-DA scores show the separation of the groups with R2Y values = 0.99 and Q2 = 0.99. This result suggests that the model explains 99% of the Y variations, with a predictive ability of 99%, indicating that the model is well established and has an excellent prediction. To identify the possible chemical markers, we used the importance of projection (VIP) and S-Plot, which were obtained from OPLS-DA analyzes for all samples. VIP is a way of classifying the best range at which discriminatory metabolites are inserted and are considered statistically significant when the value is greater than 1.0 (Ni et al., 2008). In this work, we used a VIP > 5 and $p < 0.05$.

In the S-Plot graph (Fig. 3 (b)), each point represents an ion (pair t_R-*m/z*). The X-axis represents the variable contribution, and the more the point of the t_R-*m/z* pair moves away from zero, the more it contributes to the difference between the two groups. The Y-axis represents the variable confidence, and the pair t_R-*m/z* moves away from zero, the confidence level for the difference between the two groups (Sousa et al., 2017).

According to the S-Plot (Fig. 3 (b)), the ions in the lower-left corner, represented by **4**, **6**, **7**, **9**, **15,** and **20** (Table 1), were the ions that most contributed to characterize the samples of *S. mombin* leaves. On the other hand, in the upper right corner of the S-Plot graph (Fig. 3 (b)), more characteristic ions of *S. tuberosa* leaves were identified as **5**, **18,** and **25**. Therefore, the set of ions represented by **4**, **5, 6**, **7**, **9**, **15**, **18**, **20** and **25**, are the potential biomarkers responsible for characterizing and discriminating the two groups of samples and consequently distinguish the samples of leaves of *S. mombin* and *S. tuberosa*.

As previously mentioned, each point corresponds to a pair of t_R-*m/z*, and carrying are assigned to the identified compounds. Thus, the compounds were tentatively identified as chlorogenic acid (**4**), not identified (**5**), geraniin (**6**), corilagin (**7**), not identified (**9**), galloyl-bis-HHDP-glucose (**15**), rutin (**18**), myricetin-3-*O*-rhamnoside (**20**) and kaempferol deoxyhexosyl hexoside (**25**).

3.2.2.1. Evaluation of the distribution of biomarkers in the leaves of S. mombin and S. tuberosa. In Fig. 3 (c), we can observe the average variation of the biomarkers distributed in the leaves of *S. mombin* concerning the leaves of *S. tuberosa* and vice-versa. With this, we can see what was predicted by the S-Plot and trend graphs, where we can observe and determine the biomarkers associated with the samples of *S. mombin* and *S. tuberosa* leaves.

Evaluating the mean distribution of the discriminant biomarkers of the samples of the *S. mombin*, Fig. 3(c), it is possible to observe that the compounds chlorogenic acid, geraniin, corilagin, not identified, galloyl-bis-HHDP-glucose and myricetin-3-*O*-rhamnoside practically nonexistent in the samples of leaves of *S. tuberosa*. Therefore, the compounds are

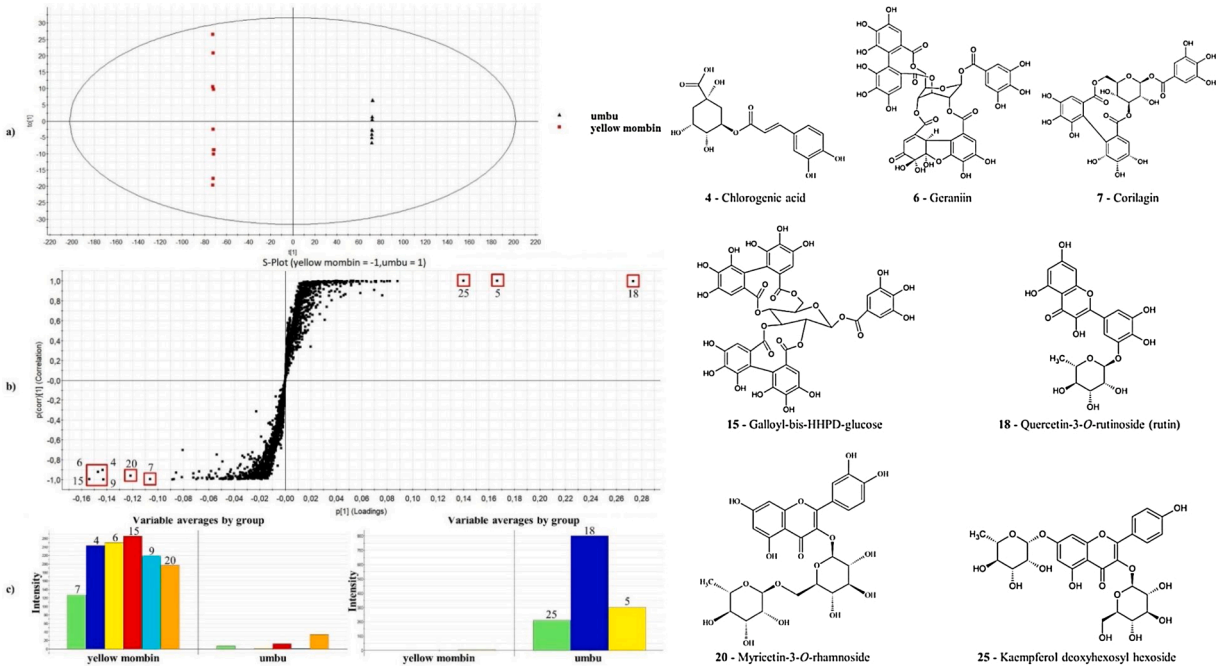

Fig. 3. Charts for the extracts of the leaves of *S. mombin* (yellow mombin) and *S. tuberosa* (umbu): (a) OPLS-DA; (b) S-Plot and (c) mean variation of the biomarkers of the hydroethanolic extract of the leaves from the *S. mombin* about the *S. tuberosa* and *S. tuberosa* about the *S. mombin*.

very characteristic of the *S. mombin* leaves.

In a similar way to that realized for the samples of leaves of *S. mombin* to the leaves of *S. tuberosa*. Evaluating the mean distribution of discriminant biomarkers of *S. tuberosa* leaves samples (Fig. 3(c)) it is possible to infer that the compounds kaempferol deoxyhexosyl hexoside, rutin, and an unidentified compound are much more widely distributed in the samples of *S. tuberosa* leaves. The chemical marker rutin stands out with the other markers, where we can observe that the same one is presented of quite an intense form in the set of samples of leaves of *S. tuberosa*.

To corroborate and confirm the inferences obtained through the graphs shown in Fig. 3(b), we can observe the trend graphs of the potential biomarkers of the leaves of *S. mombin* and *S. tuberosa* (Fig. 4). In the trend graphs, we can evaluate the dispersion of the biomarkers in the sample sets of *S. mombin* and *S. tuberosa* leaves.

In Fig. 4(a), presents the trend graphs of characteristic biomarkers of the *S. mombin* leaves. With this, we can observe the variation of biomarkers in the *S. mombin* and *S. tuberosa* leaves. Thus, as expected, biomarkers occur at higher concentrations in the *S. mombin* leaves than in the *S. tuberosa* leaves. Thus, reinforcing the conclusions obtained utilizing the S-Plot graph and the chemical distribution of the markers, where the compounds chlorogenic acid, geraniin, corilagin, not identified, galloyl-bis-HHDP-glucose and myricetin-3-*O*-rhamnoside, are the compounds responsible for characterizing and discriminating the set of *S. mombin* samples from *S. tuberosa* samples.

Analogously to what has been said previously for the samples of *S. mombin*, in Fig. 4(b), shows the trend graphs of biomarkers characteristic of *S. tuberosa* leaves. Where we can visualize the variation of the biomarkers on the *S. tuberosa* and *S. mombin* leaves. Thus, it is observed that the compounds kaempferol deoxyhexosyl hexoside, rutin, and another unidentified compound are present in higher concentrations in the *S. tuberosa* leaves samples than in the *S. mombin* leaves samples.

3.3. Evaluation of the cytotoxic activity of leaf extracts of S. mombin and S. tuberosa

Through the cytotoxic tests, it was possible to compare the efficacy of extracts of *S. mombin and S. tuberosa* leaves against the tumor and non-tumor cell lines. The extracts of *S. tuberosa* showed low cytotoxicity against the tumor lines tested. On the other hand, the extracts of *S. mombin* presented percentage that varied of high (75-100%) to moderate (51-74%) of cell growth inhibition, with values varying from 7,4 to 87,6%. The *S. mombin* extract presented a high percentage of inhibition for the leukemic lineage (HL60) (87,6%) and moderate cytotoxic activity for melanoma (B16F10) with the percentage of the 72,6%. The extracts of *S. mombin and S. tuberosa* were tested against the non-tumoral lineage, where it can be verified that the percentage of inhibition was less than 60%, therefore presenting low toxicity to the non-tumor cells (Fig. 5). Thus, through the cytotoxicity tests, it is possible to observe that the extracts of the leaves of *S. mombin* presented better activity against the leukemic lineage and melanoma, also, it is still observed that the extract presents low toxicity. These facts may be associated with the biomarkers attributed to the leaves of *S. mombin*, considering that they are the compounds responsible for the distinction of the leaves of *S. mombin* and *S. tuberosa* leaves.

It is important to mention that the biomarkers determined for the leaves of *S. mombin*, have important bioactive properties proven. The chlorogenic acid is a known bioactive agent, acting in the prevention of some disorders, including cardiovascular disorders, neurological diseases, and cancer. This compound is also capable of improving glucose tolerance and promoting weight loss (Forino et al., 2015). Studies have shown that chlorogenic acid promotes cell death by apoptosis in leukemic cells (HL60) (Yen et al., 2018). Besides, the biomarkers also have cytotoxic action against breast cancer strains (MCF7) (El-Nabi et al., 2018), as well as induction of cell death in contralateral tumors *in vivo* (Vancsik et al., 2018).

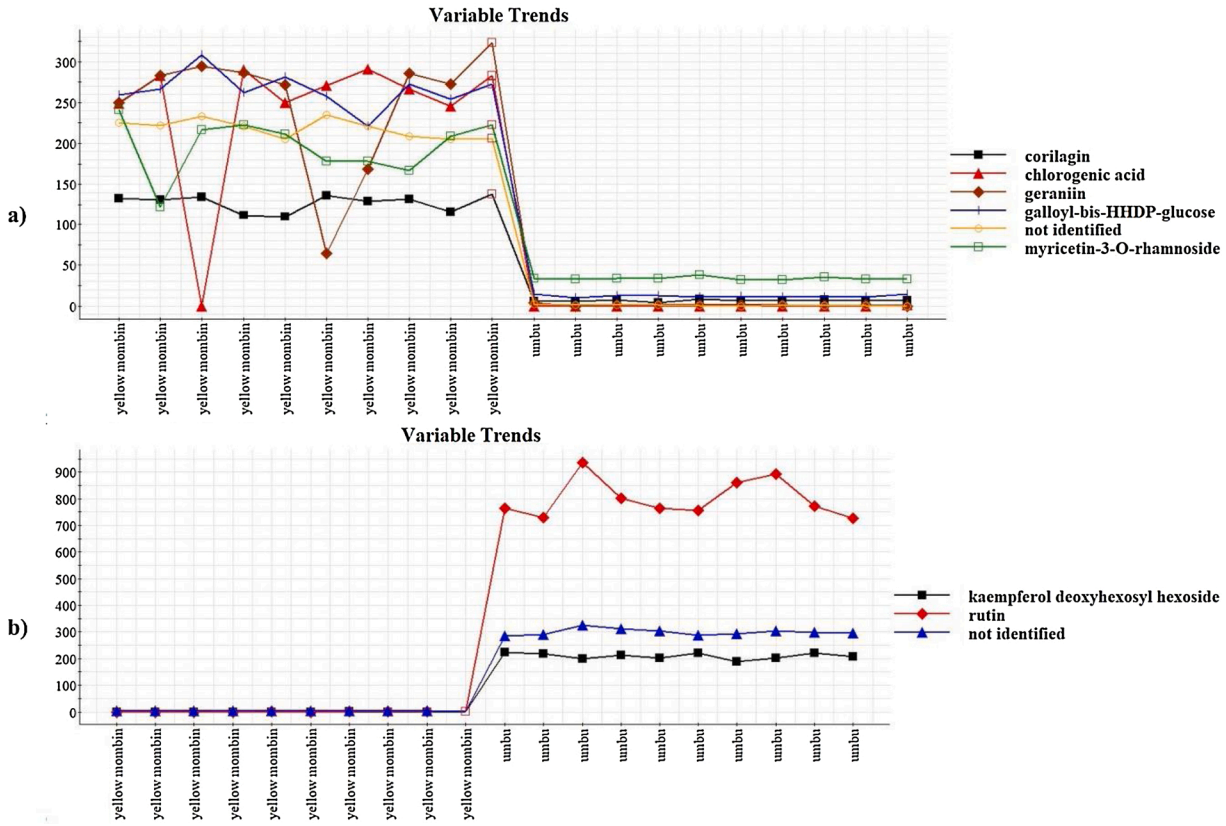

Fig. 4. Graphs of the trend variables of the chemical markers: (a) *S. mombin leaves* (yellow mombin) and (b) *S. tuberosa* leaves (umbu).

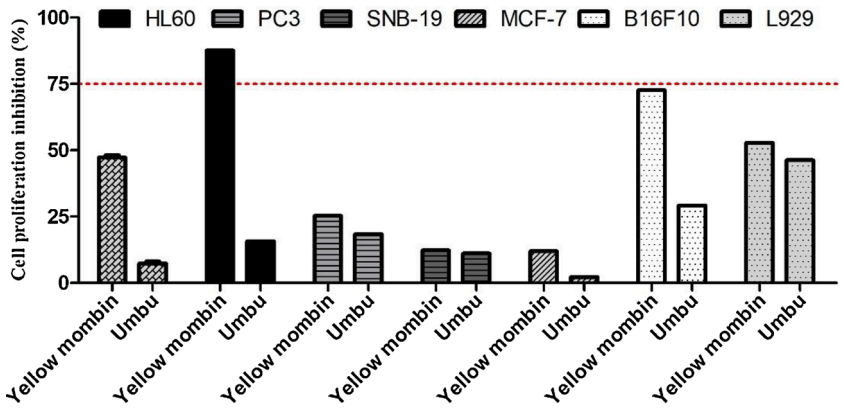

Fig. 5. Cell proliferation inhibition (%) of extracts of *Spondias* leaves determined by MTT assay after 72 h of incubation at a concentration of 100 μg mL^{-1}.

The geraniin chemical marker is an important bioactive compound in which it is related to multiple activities, such as anticancer, antiviral, antihypertensive, antihyperglycemic, and analgesic (Perera et al., 2015). The geraniin has been reported to inhibit the invasion of human osteosarcoma cells (Wang et al., 2017), induction of apoptosis in breast and lung cancer cells (MCF7) and stop the cycle in the S phase at of 24, 48 and 73 hours (Li et al., 2013; Zhai et al., 2016). The apoptotic activity of geraniin was studied in melanoma cells, where it was verified that the induction of apoptosis of this compound can provide a fundamental mechanism for the chemopreventive action of cancer (Lee et al., 2008).

The chemical marker galloyl-bis-HHDP-glucose is a tannin belonging to the class of ellagitannins. Plants rich in this class of compounds are used in traditional medicine to treat various diseases such as diarrhea, high blood pressure, rheumatism, bleeding burns, stomach problems (heartburn, nausea, gastritis, and gastric ulcer), kidney problems, urinary system and inflammatory processes in general. Besides, *in vitro* tests detected several pharmacological activities. Among them, we can mention the bactericidal, fungicidal, antiviral, cytotoxic, and healing actions (Serrano et al., 2009). In the literature consulted, there were no reports of the correlation of this compound with cytotoxicity activity.

The results of the present study demonstrate that the ethanolic extract of *S. mombin* leaves presented better cytotoxic activity against the melanoma and leukemia lines, besides presenting low toxicity to the non-tumoral lineage. Therefore, it is a candidate for a phyto-compound as a potential antitumor agent.

3.4. Theoretical results

The theoretical study was aimed to help find evidence that could probe the pharmacological activity of the main substances found in the ethanolic extract of *S. mombin* leaves. They were carried out the geometry optimization of chlorogenic acid, geraniin, and myricetin-3-*O*-rhamnoside. For comparison reasons we decided to repeat all theoretical procedures with well-known and commercial available active principles used against leukemia and other cancer lines, we have chosen doxorubicin and paclitaxel as they present obvious structural similarities with

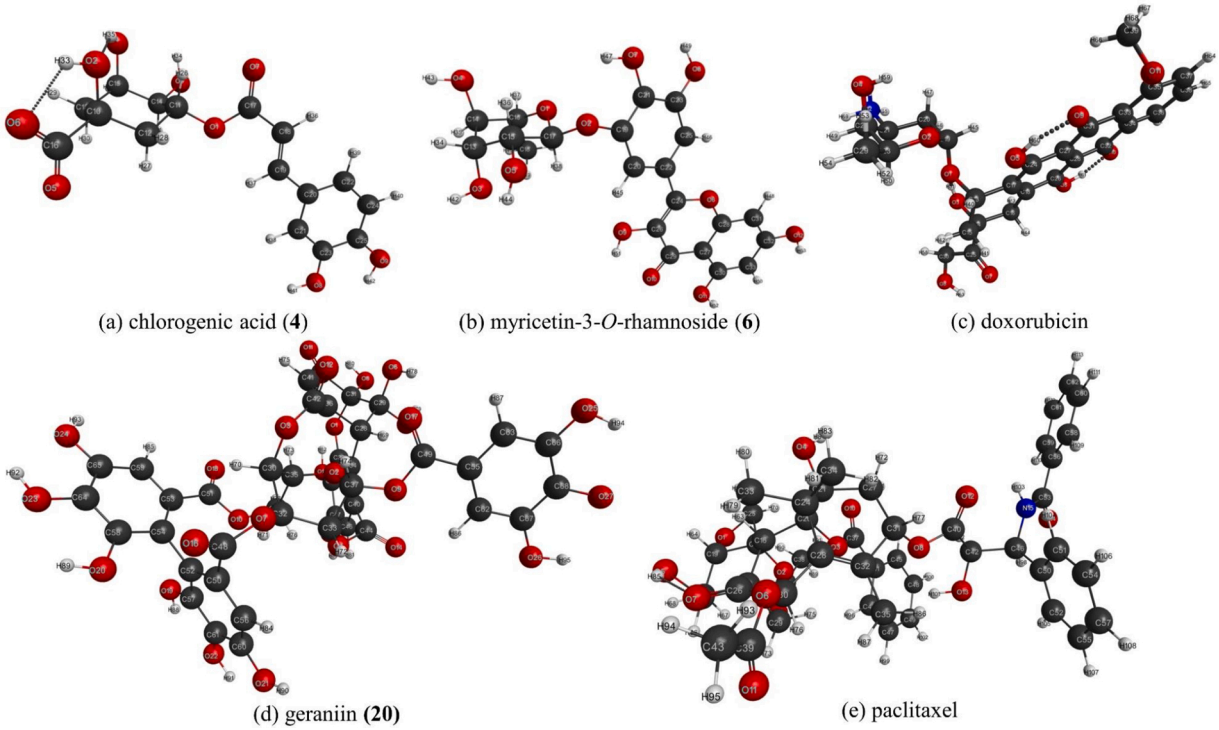

Fig. 6. Labeled molecular structure of (a) chlorogenic acid **(4)**, (b) myricetin-3-*O*-rhamnoside **(20)**, (c) doxorubicin, (d) geraniin **(6)** and (e) paclitaxel. They were optimized (DFT/ωB97X-D/6-311++G(d,p)) under the effect of solvent (water) via implicit model C-PCM.

the studied substances. The optimized structures can be seen in Fig. 6.

Regarding the similarities previously pointed out we could highlight the saturated six-member ring for the three first structures of Fig. 6 a) **(4)**, b **(20)**, and c), where **(6)** and doxorubicin have a tetrahydropyran ring. Another characteristic that must be mentioned is the ester (for **(4)**) and ether (for **(20)** and doxorubicin) linkages, respectively represented by C11-O1-C17, C17-O2-C19, and C13-O1-C19. On the other hand, d **(6)** and e, are similar in the polycyclic structure and both have important ester linkages on those cases involving C37-O9-C49 and C31-O8-C40 for **(6)** and paclitaxel, respectively.

Another possible comparison that we have made involves the frontier orbital LUMO of each compound. Fukui et al., 1954; Fukui et al., 1952 postulated that the reactivity or selectivity of some organic reactions should be controlled by the interactions between highest occupied molecular orbital (HOMO) and lowest unoccupied molecular orbital (LUMO), so one could study a mechanism in the basis of his frontier molecular orbital theory. In special cases one could refer to an active site of an enzyme or some biological receptor as a nucleophilic cavity, where often they have amino acids residues stereochemically placed to break or making bonds, in these cases, it would be fair imagine the substrate molecule as the target of the nucleophilic electron cloud in some kind of mechanisms (Náray-Szabó and Warshel, 2006), so if the interest is to compare the efficiency of some compound in produce a pharmacological effect, we could compare the lowest unoccupied molecular orbital of each comparison candidate to see if at least they have the same LUMO. The Fig. 7 shows the LUMO for each of the studied molecules.

As we see in Fig. 7, all studied structures and their commercially available comparative have a very similar orbital distribution indicating that all them start the mechanism of pharmacological action in the same way directing the LUMO density to the cavity of the active site of the enzyme or proteic receptor. For (4), (20) and doxorubicin, the six-member saturated ring should be placed out of the reactive cavity of the protein, and now it could be speculated that the sensitive part of those molecules is their ester (for **(4)**) and ether (for **(20)** and doxorubicin) linkages (respectively O1-C17, C17-O2-C19, and C13-O1-C19) that could be broken by the protein and shoot the pharmacological signal. The same could be said for **(6)** and paclitaxel, referring to their ester linkages C37-O9-C49 and C31-O8-C40, respectively.

4. Conclusions

Using the UPLC-ESI-QTOF-MS^E technique it was possible to conceive the annotation of a total of 43 compounds in the leaves of *S. tuberosa* and *S. mombin*. In this way, it was possible to establish the metabolic fingerprint, besides, it is important to mention that some compounds determined in the present work were described for the first time in *S. tuberosa* and *S. mombin*. Therefore, the present research presents itself as a great source of information for the development of future works.

The chemometric methods (PCA, OPLS-DA, and S-Plot) were essential to identify the differences inherent in the metabolic fingerprint of *S. tuberosa* and *S. mombin* leaves. Besides, these methods helped to identify the biomarkers (chlorogenic acid, geraniin, corilagin, galloyl-bis-HHPD-glucose, rutin, myricetin-3-*O*-rhamnoside e kaempferol deoxyhexosyl hexoside) responsible for characterizing and discriminating samples of the *S. tuberosa* and *S. mombin*.

Concerning the cytotoxicity tests, it was possible to observe that the extracts of the leaves of *S. mombin* showed better activity against the leukemic lineage and melanoma, also, it is still observed that the extract presents low toxicity against the non-tumoral lineage. The best cytotoxic activity obtained in the *S. mombin* leaves samples may be associated with the chemical markers, since they are responsible for distinguishing the samples of *S. mombin* and *S. tuberosa* leaves, in addition, the determined biomarkers have several pharmacological properties already mentioned in literature.

In collaboration with the correlation cytotoxic activity/biomarker, the *in silico* approach was used, where commercial drugs were compared with the biomarkers determined in this study. With this, it was verified that the biomarkers present chemical similarities with the commercial drugs used as a comparison parameter.

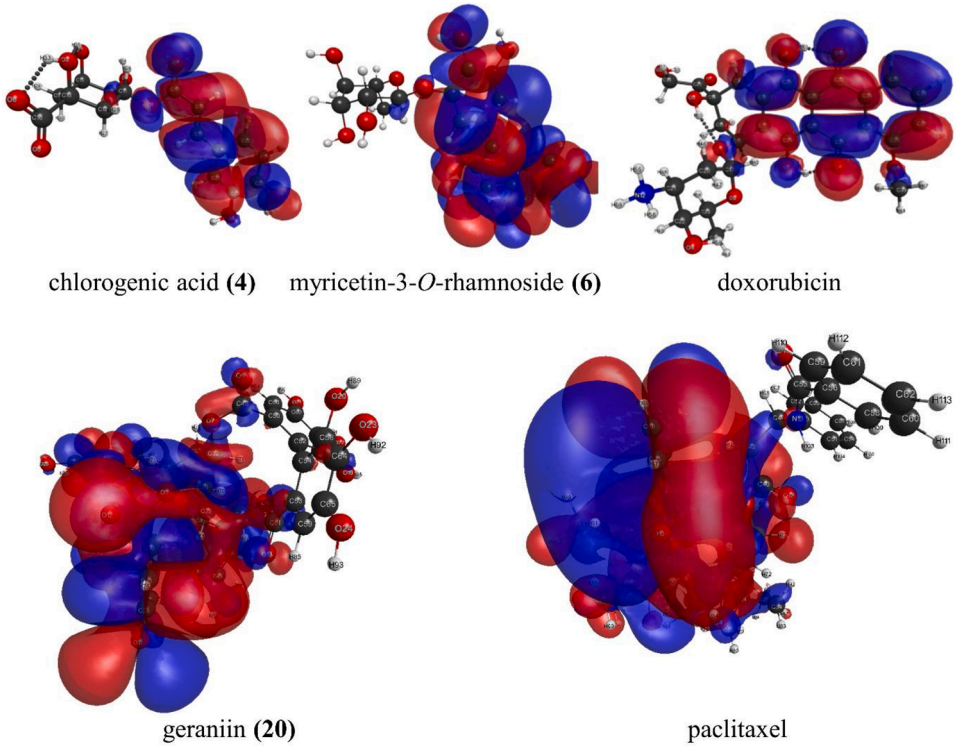

Fig. 7. Lowest unoccupied molecular orbital (LUMO) for **(4)**, **(6)**, doxorubicin, **(20)** and paclitaxel. The LUMO for each structure was calculated from the optimized (DFT/ωB97X-D/6-311++G(d,p)) structures under the effect of solvent (water) via implicit model C-PCM.

Declaration of Competing Interest

The authors report no declarations of interest.

Acknowledgments

This study was financed in part by the Coordenação de Aperfeiçoamento de Pessoal de Nível Superior - Brasil (CAPES) - Finance Code 001.

The authors gratefully acknowledge financial support from the CNPq, National Council for Scientific and Technological Development (303791/2016-0), INCT BioNat, National Institute of Science and Technology (grant # 465637/2014-0). This research was supported by resources supplied by the Center for Scientific Computing (NCC/GridUNESP) of the São Paulo State University (UNESP). We would also like to thank Embrapa (SEG 03.14.01.012.00.00).

Appendix A. Supplementary data

Supplementary material related to this article can be found, in the online version, at doi:https://doi.org/10.1016/j.phytol.2020.09.003.

References

Abu-reidah, I.M., Ali-shtayeh, M.S., Jamous, R.M., Arráez-Román, D., Segura-carretero, A., 2015. HPLC-DAD-ESI-MS/MS screening of bioactive components from *Rhus coriaria* L. (Sumac) fruits. Food Chem. 166, 179–191. https://doi.org/10.1016/j.foodchem.2014.06.011.

Agra, M. de F., Freitas, P.F. de, Barbosa-Filho, J.M., 2007. Synopsis of the plants known as medicinal and poisonous in Northeast of Brazil. Rev. Bras. Farmacogn. 17, 114–140. https://doi.org/10.1590/S0102-695X2007000100021.

Ajao, A.O., Shonukan, O., Femi-onadeko, B., 1985. Antibacterial Effect of Aqueous and Alcohol Extracts of *Spondias mombin*, and *Alchornea cordifolia* - Two Local Antimicrobial Remedies. Int. J. Crude Drug Res. 23, 67–72. https://doi.org/10.3109/13880208509069004.

Barone, V., Cossi, M., 1998. Quantum Calculation of Molecular Energies and Energy Gradients in Solution by a Conductor Solvent Model. J. Phys. Chem. A 102, 1995–2001. https://doi.org/10.1021/jp9716997.

Bataglion, G.A., da Silva, F.M.A., Eberlin, M.N., Koolen, H.H.F., 2015. Determination of the phenolic composition from Brazilian tropical fruits by UHPLC–MS/MS. Food Chem. 180, 280–287. https://doi.org/10.1016/j.foodchem.2015.02.059.

Bode, B.M., Gordon, M.S., 1998. Macmolplt: a graphical user interface for GAMESS. J. Mol. Graph. Model. 16, 133–138. https://doi.org/10.1016/S1093-3263(99)00002-9.

Cabral, B., Siqueira, E.M.S., Bitencourt, M.A.O., Lima, M.C.J.S., Lima, A.K., Ortmann, C. F., Chaves, V.C., Fernandes-pedrosa, M.F., Rocha, H.A.O., Scortecci, K.C., Reginatto, F.H., Giordani, R.B., Zucolotto, S.M., 2016. Phytochemical study and anti-inflammatory and antioxidant potential of *Spondias mombin* leaves. Rev. Bras. Farmacogn. 26, 304–311. https://doi.org/10.1016/j.bjp.2016.02.002.

Chagas-Paula, D.A., Zhang, T., Da Costa, F.B., Edrada-Ebel, R.A., 2015. A Metabolomic Approach to Target Compounds from the Asteraceae Family for Dual COX and LOX Inhibition. Metabolites 5, 404–430. https://doi.org/10.3390/metabo5030404.

Chai, J.-D., Head-Gordon, M., 2008. Long-range corrected hybrid density functionals with damped atom–atom dispersion corrections. Phys. Chem. Chem. Phys. 10, 6615. https://doi.org/10.1039/b810189b.

Corthout, J., Pieters, L.A., Claeys, M., Vanden Berghe, D.A., Vlietinck, A.J., 1991. Antiviral ellagitannins from *Spondias mombin*. Phytochemistry 30, 1129–1130. https://doi.org/10.1016/S0031-9422(00)95187-2.

Cossi, M., Barone, V., Cammi, R., Tomasi, J., 1996. Ab initio study of solvated molecules: a new implementation of the polarizable continuum model. Chem. Phys. Lett. 255, 327–335. https://doi.org/10.1016/0009-2614(96)00349-1.

Cunha, A.G., Brito, E.S., Moura, C.F.H., Ribeiro, P.R.V., Miranda, M.R.A., 2017. UPLC-qTOF-MS/MS-based phenolic profile and their biosynthetic enzyme activity used to discriminate between cashew apple (*Anacardium occidentale* L.) maturation stages. J. Chromatogr. B 1051, 24–32. https://doi.org/10.1016/j.jchromb.2017.02.022.

Dias, J.L., Mazzutti, S., de Souza, J.A.L., Ferreira, S.R.S., Soares, L.A.L., Stragevitch, L., Danielski, L., 2019. Extraction of umbu (*Spondias tuberosa*) seed oil using CO2, ultrasound and conventional methods: Evaluations of composition profiles and antioxidant activities. J. Supercrit. Fluids 145, 10–18. https://doi.org/10.1016/j.supflu.2018.11.011.

Dorta, E., González, M., Lobo, M.G., Sánchez-Moreno, C., de Ancos, B., 2014. Screening of phenolic compounds in by-product extracts from mangoes (*Mangifera indica* L.) by HPLC-ESI-QTOF-MS and multivariate analysis for use as a food ingredient. Food Res. Int. 57, 51–60. https://doi.org/10.1016/j.foodres.2014.01.012.

Dou, J., Lee, V.S.Y., Tzen, J.T.C., Lee, M.-R., 2007. Identification and Comparison of Phenolic Compounds in the Preparation of Oolong Tea Manufactured by Semifermentation and Drying Processes. J. Agric. Food Chem. 55, 7462–7468. https://doi.org/10.1021/jf0718603.

El-Nabi, S.E.-S.H., Dawoud, G.T.M., El-Garawani, I.M., El Shafey, S.S., 2018. HPLC analysis of phenolic acids, antioxidant activity and in vitro effectiveness of green and roasted Caffea arabica bean extracts: a comparative study. Anticancer. Agents Med. Chem. 18. https://doi.org/10.2174/1871520618666180124121927.

Engels, C., Gräter, D., Esquivel, P., Jiménez, V.M., Gänzle, M.G., Schieber, A., 2012. Characterization of phenolic compounds in jocote (*Spondias purpurea* L.) peels by ultra high-performance liquid chromatography/electrospray ionization mass spectrometry. Food Res. Int. 46, 557–562. https://doi.org/10.1016/j.foodres.2011.04.003.

Erşan, S., Güçlü Üstündağ, Ö., Carle, R., Schweiggert, R.M., 2016. Identification of phenolic compounds in red and green pistachio (*Pistacia vera* L.) hulls (exo- and mesocarp) by HPLC-DAD-ESI-(HR)-MSn. J. Agric. Food Chem. 64, 5334–5344. https://doi.org/10.1021/acs.jafc.6b01745.

Farag, M.A., Mohsen, M., Heinke, R., Wessjohann, L.A., 2014. Metabolomic fingerprints of 21 date palm fruit varieties from Egypt using UPLC/PDA/ESI–qTOF-MS and GC–MS analyzed by chemometrics. Food Res. Int. 64, 218–226. https://doi.org/10.1016/j.foodres.2014.06.021.

Forino, M., Tenore, G.C., Tartaglione, L., Carmela, D., Novellino, E., Ciminiello, P., 2015. (1S,3R,4S,5R)5-*O*-Caffeoylquinic acid: Isolation, stereo-structure characterization and biological activity. Food Chem. 178, 306–310. https://doi.org/10.1016/j.foodchem.2015.01.109.

Fracassetti, D., Costa, C., Moulay, L., Tomás-barberán, F.A., 2013. Ellagic acid derivatives, ellagitannins, proanthocyanidins and other phenolics, vitamin C and antioxidant capacity of two powder products from camu-camu fruit (*Myrciaria dubia*). Food Chem. 139, 578–588. https://doi.org/10.1016/j.foodchem.2013.01.121.

Fukui, K., Yonezawa, T., Nagata, C., Shingu, H., 1954. Molecular Orbital Theory of Orientation in Aromatic, Heteroaromatic, and Other Conjugated Molecules. J. Chem. Phys. 22, 1433–1442. https://doi.org/10.1063/1.1740412.

Fukui, K., Yonezawa, T., Shingu, H., 1952. A Molecular Orbital Theory of Reactivity in Aromatic Hydrocarbons. J. Chem. Phys. 20, 722–725. https://doi.org/10.1063/1.1700523.

Gomes, E.D.B., Ramalho, S.A., Gualberto, N.C., Miranda, R. de C.M. de, Nigam, N., Narain, N., 2013. A Rapid Method for Determination of Some Phenolic Acids in Brazilian Tropical Fruits of Mangaba (*Hancornia speciosa* Gomes) and Umbu (*Spondias tuberosa* Arruda Camara) by UPLC. J. Anal. Sci. Methods Instrum. 03, 1–10. https://doi.org/10.4236/jasmi.2013.33A001.

Gomes, M., Lins, R.D.A.U., Langassner, S.M.Z., Silveira, É.J.D. da, Carvalho, T.G. de, Lopes, M.L.D. de S., Araújo, L. de S., Medeiros, C.A.C.X. de, Leitão, R.F. de C., Guerra, G.C.B., Junior, R.F. de A., Araújo, A.A. de, 2020. Anti-inflammatory and antioxidant activity of hydroethanolic extract of *Spondias mombin* leaf in an oral mucositis experimental model. Arch. Oral Biol. 111, 104664 https://doi.org/10.1016/j.archoralbio.2020.104664.

González-Riano, C., Dudzik, D., Garcia, A., Gil-De-La-Fuente, A., Gradillas, A., Godzien, J., López-Gonzálvez, ángeles, Rey-Stolle, F., Rojo, D., Ruperez, F.J., Saiz, J., Barbas, C., 2020. Recent developments along the analytical process for metabolomics workflows. Anal. Chem. 92, 203–226. https://doi.org/10.1021/acs.analchem.9b04553.

Guedes, J., Alves Filho, E., Silva, M., Rodrigues, T., Ramires, C., Lima, M., Silva, G., Pessoa, C., Canuto, K., Brito, E., Alves, R., Nascimento, R., Zocolo, G., 2020. GC-MS-Based Metabolomic Profiles Combined with Chemometric Tools and Cytotoxic Activities of Non-Polar Leaf Extracts of *Spondias mombin* L. and *Spondias tuberosa* Arr. Cam. J. Braz. Chem. Soc. 1–10. https://doi.org/10.21577/0103-5053.20190185, 00.

Guedes, J.A.C., Alves Filho, E. de G., Rodrigues, T.H.S., Silva, M.F.S., Souza, F.V.D., Silva, L.M.A. e, Alves, R.E., Canuto, K.M., Brito, E.S. de, Pessoa, C. do Ó., Nascimento, R.F., Zocolo, G.J., 2018. Metabolic profile and cytotoxicity of non-polar extracts of pineapple leaves and chemometric analysis of different pineapple cultivars. Ind. Crops Prod. 124, 466–474. https://doi.org/10.1016/j.indcrop.2018.08.026.

Hajdu, Z., Hohmann, J., 2012. An ethnopharmacological survey of the traditional medicine utilized in the community of Porvenir, Bajo Paraguá Indian Reservation. Bolivia. J. Ethnopharmacol. 139, 838–857. https://doi.org/10.1016/j.jep.2011.12.029.

Hanhineva, K., Rogachev, I., Kokko, H., Mintz-Oron, S., Venger, I., Kärenlampi, S., Aharoni, A., 2008. Non-targeted analysis of spatial metabolite composition in strawberry (*Fragaria* × *ananassa*) flowers. Phytochemistry 69, 2463–2481. https://doi.org/10.1016/j.phytochem.2008.07.009.

Kim, S., Thiessen, P.A., Bolton, E.E., Chen, J., Fu, G., Gindulyte, A., Han, L., He, J., He, S., Shoemaker, B.A., Wang, J., Yu, B., Zhang, J., Bryant, S.H., 2016. PubChem Substance and Compound databases. Nucleic Acids Res. 44, D1202–D1213. https://doi.org/10.1093/nar/gkv951.

Kumar, S., Chandra, P., Bajpai, V., Singh, A., Srivastava, M., Mishra, D.K., Kumar, B., 2015. Rapid qualitative and quantitative analysis of bioactive compounds from *Phyllanthus amarus* using LC/MS/MS techniques. Ind. Crops Prod. 69, 143–152. https://doi.org/10.1016/j.indcrop.2015.02.012.

Lee, J.-C., Tsai, C.-Y., Kao, J.-Y., Kao, M.-C., Tsai, S.-C., Chang, C.-S., Huang, L.-J., Kuo, S.-C., Lin, J.-K., Way, T.-D., 2008. Geraniin-mediated apoptosis by cleavage of focal adhesion kinase through up-regulation of Fas ligand expression in human melanoma cells. Mol. Nutr. Food Res. 52, 655–663. https://doi.org/10.1002/mnfr.200700381.

Li, J., Wang, S., Yin, J., Pan, L., 2013. Geraniin induces apoptotic cell death in human lung adenocarcinoma A549 cells *in vitro* and *in vivo*. Can. J. Physiol. Pharmacol. 91, 1016–1024. https://doi.org/10.1139/cjpp-2013-0140.

Liu, X., Zhou, L., Shi, X., Xu, G., 2019. New advances in analytical methods for mass spectrometry-based large-scale metabolomics study. TrAC - Trends Anal. Chem. 121, 115665 https://doi.org/10.1016/j.trac.2019.115665.

Mosmann, T., 1983. Rapid colorimetric assay for cellular growth and survival: Application to proliferation and cytotoxicity assays. J. Immunol. Methods 65, 55–63. https://doi.org/10.1016/0022-1759(83)90303-4.

Náray-Szabó, G., Warshel, A., 2006. Computational Approaches to Biochemical Reactivity. Springer Science & Business Media, Netherlands.

Nehme, C.J., Moraes, P.L.R. De, Tininis, A.G., Cavalheiro, A.J., 2008. Intraspecific variability of flavonoid glycosides and styrylpyrones from leaves of *Cryptocarya mandioccana* Meisner (Lauraceae). Biochem. Syst. Ecol. 36, 602–611. https://doi.org/10.1016/j.bse.2008.05.001.

Neto, E.M. de F.L., Peroni, N., Albuquerque, U.P. De, 2010. Traditional Knowledge and Management of Umbu (*Spondias tuberosa*, Anacardiaceae): An Endemic Species from the Semi–Arid Region of Northeastern Brazil. Econ. Bot. 64, 11–21. https://doi.org/10.1007/s12231-009-9106-3.

Ni, Y., Su, M., Lin, J., Wang, X., Qiu, Y., Zhao, A., Chen, T., Jia, W., 2008. Metabolic profiling reveals disorder of amino acid metabolism in four brain regions from a rat model of chronic unpredictable mild stress. FEBS Lett. 582, 2627–2636. https://doi.org/10.1016/j.febslet.2008.06.040.

Pereira, C., Oliveira, L.L. de, Gonçalves, R., Amaral, A.C.F., Kuster, R.M., Sakuragui, C. M., 2015. Phytochemical and phylogenetic analysis of *Spondias* (Anacardiaceae). Quim. Nova 38, 813–816. https://doi.org/10.5935/0100-4042.20150087.

Perera, A., Ton, S.H., Palanisamy, U.D., 2015. Perspectives on geraniin, a multifunctional natural bioactive compound. Trends Food Sci. Technol. 44, 243–257. https://doi.org/10.1016/j.tifs.2015.04.010.

Pezzatti, J., Boccard, J., Codesido, S., Gagnebin, Y., Joshi, A., Picard, D., González-Ruiz, V., Rudaz, S., 2020. Implementation of liquid chromatography–high resolution mass spectrometry methods for untargeted metabolomic analyses of biological samples: A tutorial. Anal. Chim. Acta 1105, 28–44. https://doi.org/10.1016/j.aca.2019.12.062.

Rappe, A.K., Casewit, C.J., Colwell, K.S., Goddard, W.A., Skiff, W.M., 1992. UFF, a full periodic table force field for molecular mechanics and molecular dynamics simulations. J. Am. Chem. Soc. 114, 10024–10035. https://doi.org/10.1021/ja00051a040.

Sampaio, T.I. dos S, de Melo, N.C., Paiva, B.T. de F., Aleluia, G.A. da S., da Silva Neto, F. L.P., da Silva, H.R., Keita, H., Cruz, R.A.S., Sánchez-Ortiz, B.L., Pineda-Peña, E.A., Balderas, J.L., Navarrete, A., Carvalho, J.C.T., 2018. Leaves of *Spondias mombin* L. a traditional anxiolytic and antidepressant: Pharmacological evaluation on zebrafish (*Danio rerio*). J. Ethnopharmacol. 224, 563–578. https://doi.org/10.1016/j.jep.2018.05.037.

Schieber, A., Berardini, N., Carle, R., 2003. Identification of flavonol and xanthone glycosides from mango (*Mangifera indica* L. Cv. "Tommy Atkins") peels by high-performance liquid chromatography-electrospray ionization mass spectrometry. J. Agric. Food Chem. 51, 5006–5011. https://doi.org/10.1021/jf030218f.

Schmidt, M.W., Baldridge, K.K., Boatz, J.A., Elbert, S.T., Gordon, M.S., Jensen, J.H., Koseki, S., Matsunaga, N., Nguyen, K.A., Su, S., Windus, T.L., Dupuis, M., Montgomery, J.A., 1993. General atomic and molecular electronic structure system. J. Comput. Chem. 14, 1347–1363. https://doi.org/10.1002/jcc.540141112.

Serrano, J., Puupponen-Pimiä, R., Dauer, A., Aura, A.M., Saura-Calixto, F., 2009. Tannins: Current knowledge of food sources, intake, bioavailability and biological effects. Mol. Nutr. Food Res. 53, 310–329. https://doi.org/10.1002/mnfr.200900039.

Silva, A.R.A., Morais, S.M., Marques, M.M.M., Lima, D.M., Santos, S.C.C., Almeida, R.R., Vieira, I.G.P., Guedes, M.I.F., 2011. Antiviral activities of extracts and phenolic components of two *Spondias* species against dengue virus. J. Venom. Anim. Toxins Incl. Trop. Dis. 17, 406–413. https://doi.org/10.1590/S1678-91992011000400007.

Silva, R.V., Costa, S.C.C., Branco, C.R.C., Branco, A., 2016. *In vitro* photoprotective activity of the *Spondias purpurea* L. peel crude extract and its incorporation in a pharmaceutical formulation. Ind. Crops Prod. 83, 509–514. https://doi.org/10.1016/j.indcrop.2015.12.077.

Sousa, A.D., Maia, I.V., Ribeiro, P.R.V., Canuto, K.M., Zocolo, G.J., Sousa de Brito, E., 2017. UPLC-QTOF-MSE-based chemometric approach driving the choice of the best extraction process for *Phyllanthus niruri*. Sep. Sci. Technol. 52, 1696–1706. https://doi.org/10.1080/01496395.2017.1298612.

Spackman, M.A., 1996. Potential derived charges using a geodesic point selection scheme. J. Comput. Chem. 17, 1–18. https://doi.org/10.1002/(SICI)1096-987X(19960115)17:1<1::AID-JCC1>3.0.CO;2-V.

Tomás-Barberán, F.A., Clifford, M.N., 2000. Dietary hydroxybenzoic acid derivatives - nature, occurrence and dietary burden. J. Sci. Food Agric. 80, 1024–1032. https://doi.org/10.1002/(SICI)1097-0010(20000515)80:7<1024::AID-JSFA567>3.0.CO;2-S.

Tomasi, J., Mennucci, B., Cammi, R., 2005. Quantum Mechanical Continuum Solvation Models. Chem. Rev. 105, 2999–3094. https://doi.org/10.1021/cr9904009.

van den Berg, R.A., Hoefsloot, H.C.J., Westerhuis, J.A., Smilde, A.K., van der Werf, M.J., 2006. Centering, scaling, and transformations: Improving the biological information content of metabolomics data. BMC Genomics 7, 1–15. https://doi.org/10.1186/1471-2164-7-142.

Vancsik, T., Kovago, C., Kiss, E., Papp, E., Forika, G., Benyo, Z., Meggyeshazi, N., Krenacs, T., 2018. Modulated electro-hyperthermia induced loco-regional and systemic tumor destruction in colorectal cancer allografts. J. Cancer 9, 41–53. https://doi.org/10.7150/jca.21520.

Wang, Y., Wan, D., Zhou, R., Zhong, W., Lu, S., Chai, Y., 2017. Geraniin inhibits migration and invasion of human osteosarcoma cancer cells through regulation of PI3K/Akt and ERK1/2 signaling pathways. Anticancer. Drugs 28, 959–966. https://doi.org/10.1097/CAD.0000000000000535.

Wold, S., Sjöström, M., Eriksson, L., 2001. PLS-regression: a basic tool of chemometrics. Chemom. Intell. Lab. Syst. 58, 109–130. https://doi.org/10.1016/S0169-7439(01)00155-1.

Yen, G.C., Chen, C.S., Chang, W.T., Wu, M.F., Cheng, F.T., Shiau, D.K., Hsu, C.L., 2018. Antioxidant activity and anticancer effect of ethanolic and aqueous extracts of the roots of *Ficus beecheyana* and their phenolic components. J. Food Drug Anal. 26, 182–192. https://doi.org/10.1016/j.jfda.2017.02.002.

Zeraik, M.L., Queiroz, E.F., Marcourt, L., Ciclet, O., Castro-Gamboa, I., Silva, D.H.S., Cuendet, M., Bolzani, V., da, S., Wolfender, J.-L., 2016. Antioxidants, quinone reductase inducers and acetylcholinesterase inhibitors from *Spondias tuberosa* fruits. J. Funct. Foods 21, 396–405. https://doi.org/10.1016/j.jff.2015.12.009.

Zhai, J.-W., Gao, C., Ma, W.-D., Wang, W., Yao, L.-P., Xia, X.-X., Luo, M., Zu, Y.-G., Fu, Y.-J., 2016. Geraniin induces apoptosis of human breast cancer cells MCF-7 via ROS-mediated stimulation of p38 MAPK. Toxicol. Mech. Methods 26, 311–318. https://doi.org/10.3109/15376516.2016.1139025.